

MINING BLAST-INDUCED GROUND MOTIONS IN TAILINGS DAM

Leonardo Santana de Oliveira Dias ^{1*}, Marco Antônio Silva Braga ¹, Alan de Souza Cunha ¹,
Gerrit Olivier ², and Rodrigo Peluci de Figueiredo ³

ABSTRACT. Ground motions caused by routine blasting activities represent a concern for mining companies, that face the challenge of producing without causing critical damage to tailings dams, mine pit slopes and waste piles. Few dams in Brazil are monitored by microseismic systems, and there are no references in the literature about monitoring in open pit mine and dam. In order to analyze the ground motion data induced by blats and their relationship with dam stability, it was installed a seismic system, that records events continuously in an array of 16 geophones (14 Hz and 4.5 Hz), 12 installed in an open pit and 4 in a tailings dam with value measurement of Peak Ground Acceleration, Peak Ground Velocity, dominant frequency, and seismic source parameters related to blast events. In the monitored period, sensors from the open pit and dam were analyzed and all accelerations recorded showed that ~95% of the values are lower than 0.06 m/s², with 90% of the records with higher dominant frequency (>10 Hz), that presents lower damage potential due to the lower capacity to produce high values of displacements. The system showed the potential to add new data and information to the current dam geotechnical instrumentation.

Keywords: blast-induced seismicity; microseismic monitoring; tailings dam; risk management; geotechnical monitoring plan.

RESUMO. Os *ground motions* gerados pelas atividades rotineiras de detonação representam uma preocupação para as mineradoras, que enfrentam o desafio de produzir sem causar danos críticos às barragens de rejeitos, taludes de cava e pilhas de estéril. Poucas barragens no Brasil são monitoradas por sistemas microssísmicos e não há referências na literatura sobre monitoramento em cava e barragem. Para analisar os dados dos *ground motions* causados pelas detonações e a sua relação com a estabilidade de uma barragem, foi instalado um sistema de monitoramento sísmico, que registra eventos continuamente num arranjo de 16 geofones (14 Hz e 4,5 Hz), instalados 12 na cava e 4 na barragem, com medição de valores de *Peak Ground Acceleration*, *Peak Ground Velocity*, frequência dominante e parâmetros da fonte sísmica dos desmontes. No período monitorado, quando foram analisados os sensores da mina e da barragem, todas as acelerações mostraram que ~95% dos valores são menores que 0,06 m/s², com 90% dos registros com maior frequência dominante (> 10 Hz), que apresenta menor potencial de dano devido à menor capacidade de produzir altos valores de deslocamentos. O sistema mostrou potencial para agregar novos dados e informações à atual instrumentação geotécnica da barragem.

Palavras-chave: sismicidade induzida por desmontes; monitoramento microssísmico; barragem de rejeitos; gerenciamento de risco; plano de monitoramento geotécnico.

*Corresponding author: Leonardo Santana de Oliveira Dias

¹Universidade Federal do Rio de Janeiro - UFRJ, Centro de Pesquisa em Geofísica Aplicada, Rio de Janeiro, RJ, Brazil – E-mails: leonardo.santana@gmail.com, marcobraga@geologia.ufrj.br, alan.fis@gmail.com

²University of Tasmania - UTAS, Institute of Mine Seismology, Applied Geophysics, Hobart, Tasmania, Australia – E-mail: gerrit.olivier@utas.edu.au

³Universidade Federal de Ouro Preto - UFOP, Departamento de Engenharia de Minas e Núcleo de Geotecnia, Ouro Preto, MG, Brazil – E-mail: rpfigueiredo@ufop.edu.br

INTRODUCTION

Tailings dams are structures used in mining for waste disposal, often constructed with steep slopes using the coarse fraction of tailings, and with the secondary objective to store water for reuse (Nimbalkar et al., 2018; Silva, 2019). The recent mining dam failures have caused significant damage to the environment and even loss of life, bringing up the discussion about new monitoring methodologies (Olivier et al., 2017). The disasters of Fundão Dam (November, 2015) and Córrego do Feijão (January, 2019) in Minas Gerais State, Brazil, are examples of the human, social, environmental, and economic costs of tailings dam failures (Lima et al., 2020).

Dams near mining sites are exposed to ground motions from seismic waves generated by routine activities of the mine operations (e.g., blasts) and induced seismicity. These ground motions might affect the physical integrity of these structures if the vibrations are enough severe, potentially resulting in liquefaction of tailings sands and sliding collapse or failure (Shuran & Shujin, 2011). Silva-Castro (2012) defines that it is important for the mining industry to have tools and methodologies to model and predict blast vibration impacts, as well as complement traditional geotechnical monitoring (e.g., piezometers, geodetic prisms and water levels).

Seismic waves generated by blasts can be recorded as seismograms by seismic monitoring systems (Ma et al., 2017). The most common type of seismic monitoring system deployed in mines is called microseismic arrays, commonly designed to monitor vibrations near mine (Errington, 2006). Microseismic monitoring has been commonly used in underground mining operations (Mendecki et al., 2010), with numerous applications in tunnel stability, hydropower engineering, slope stability (Lijie, 2015), and natural cave integrity (Dias et al., 2016). In particular, the use of microseismic monitoring in mining dams for tailings stability has rarely been investigated, with only a few examples available in literature (Olivier et al., 2017, 2018; Wit & Olivier, 2018; Oliveira, 2021).

Modern digital microseismic monitoring technology has evolved over the past decades to

reliably record high quality continuous seismic data (Mendecki et al., 2010; Goldswain, 2020). Typically, a seismic monitoring network refers to an array of uni or triaxial sensors installed across the mine site, where seismic events (like blasts or microtremors) are recorded as a collection of seismograms. This real-time seismic monitoring network measures the tailings dam's exposure to local seismicity from blast or natural events. The network can also provide valuable information to geotechnical engineers to use in their Trigger Action Responses Plan (TARP) based on the acceleration's values recorded in the structure. In this paper, we use data acquired by a routine microseismic monitoring system installed in the B1 Dam at the Mining Chemical Complex of Cajati (São Paulo State, Brazil), to assess the blast-induced seismic vibrations recorded in the dam crest.

The Mining Chemical Complex of Cajati is mainly composed by an open pit (Mine Hill), three mine waste piles and two tailings' dams, owned and operated by Mosaic Fertilizantes (Mosaic Company). The complex is located near the city of Cajati, approximately 230 km south-west of the city of São Paulo (Fig. 1), following the road BR-116 in the direction of the city of Curitiba (Paraná State). The open pit is inserted in the Jacupiranga Alkaline Complex, a classic Brazilian occurrence of alkaline and ultrabasic rocks with associated carbonates in a phosphate deposit of magmatic affiliation (Barros, 2001; Oliveira & Sant'agostino, 2020), reaching in 2020 the production of 400,000 t of phosphate concentrate with 33.8% P_2O_5 .

Mine Hill ('Morro da Mina') operations include daily blasts and is located approximately 2 km from the B1 Dam (Fig. 2). Over the period of April 2018 to December 2019, the system recorded 176 blasts that triggered sensors installed in the dam and open pit, resulting in 463 seismograms that were analyzed and compared with the seismic design criteria.

SITE

Geological overview

Mine Hill (Morro da Mina) is inserted in the Jacupiranga Alkaline Complex, in the south-central portion of the Ribeira Belt (Mantiqueira Province).

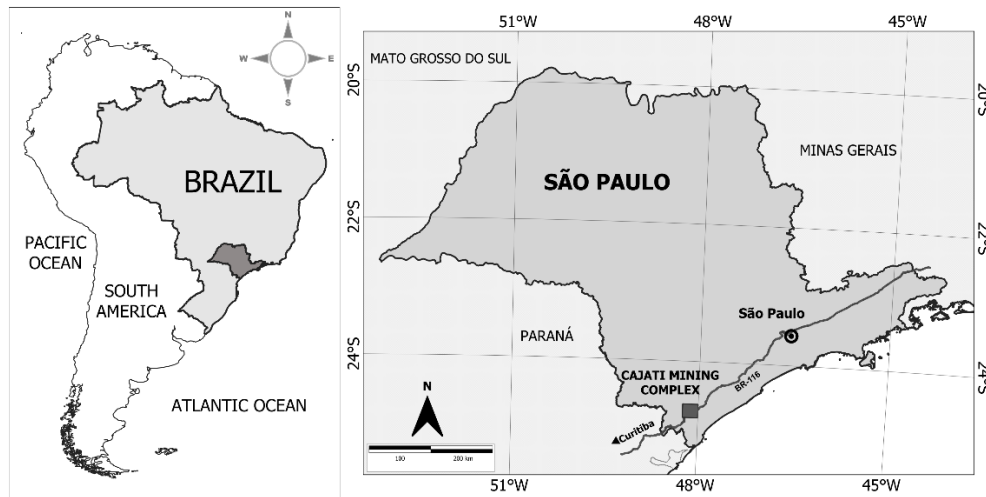


Figure 1 - Location of the Mining Chemical Complex of Cajati.

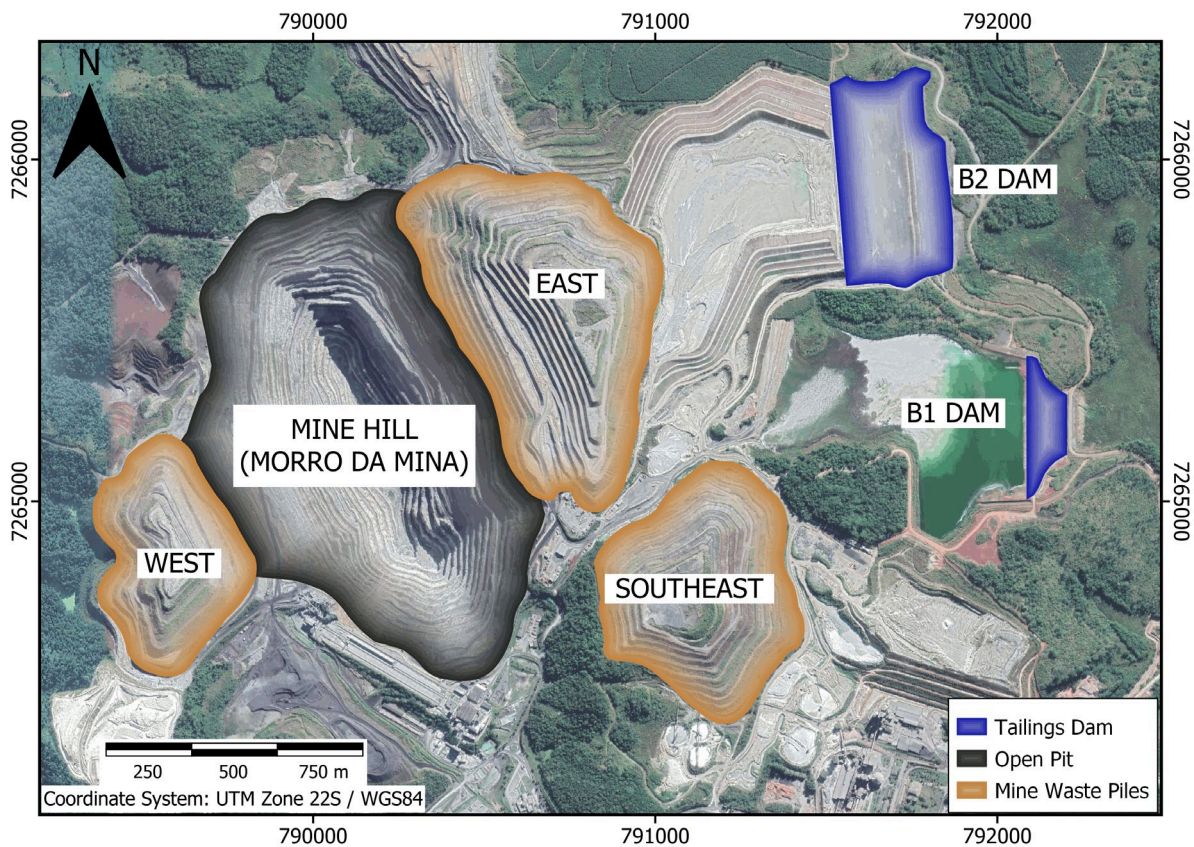


Figure 2 - View of the mining infrastructure with the location of the mine waste piles (East, West, and Southeast), Mine Hill open pit, B1 and B2 dams (image source from Google Earth 2020).

The region represents a key area in the regional tectonic context (Fig. 3), in the articulation between Luís Alves cratonic fragment and Apiaí, Curitiba and Paranaguá domains, from southern Ribeira Belt (Faleiros & Pavan, 2013).

The alkaline rocks (Jacupiranga Complex) correspond to a Mesozoic magmatism with an oval shape measuring approximately 10.5 km x 6.7 km with orientation NNW (Barros, 2001). Figure 4

shows the geological lithologies of the area, composed by clinopyroxenites (jacupiranguito) of alkaline affinity, dunites associated with carbonatites and unsaturated alkaline rocks (ijolites and melteigites), with basic terms to acids (gabbros and syenites), alkaline subvolcanic (phonolites, lamprophyres, essexites and theralites) and late metasomatic rocks (fenites) (Faleiros & Pavan, 2013).

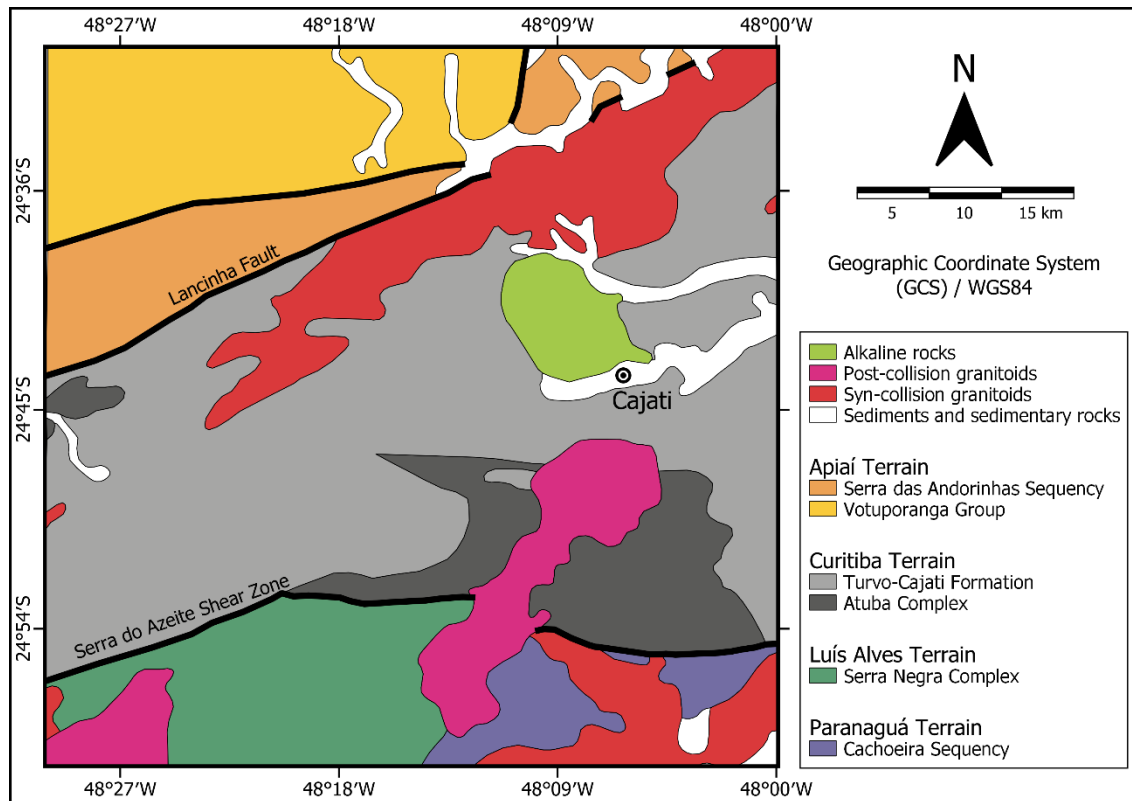


Figure 3 - Simplified tectonic map showing the relationship between Luís Alves cratonic fragment and Apiaí, Curitiba and Paranaguá domains, that are part of Ribeira Belt (modified from Faleiros & Pavan, 2013).

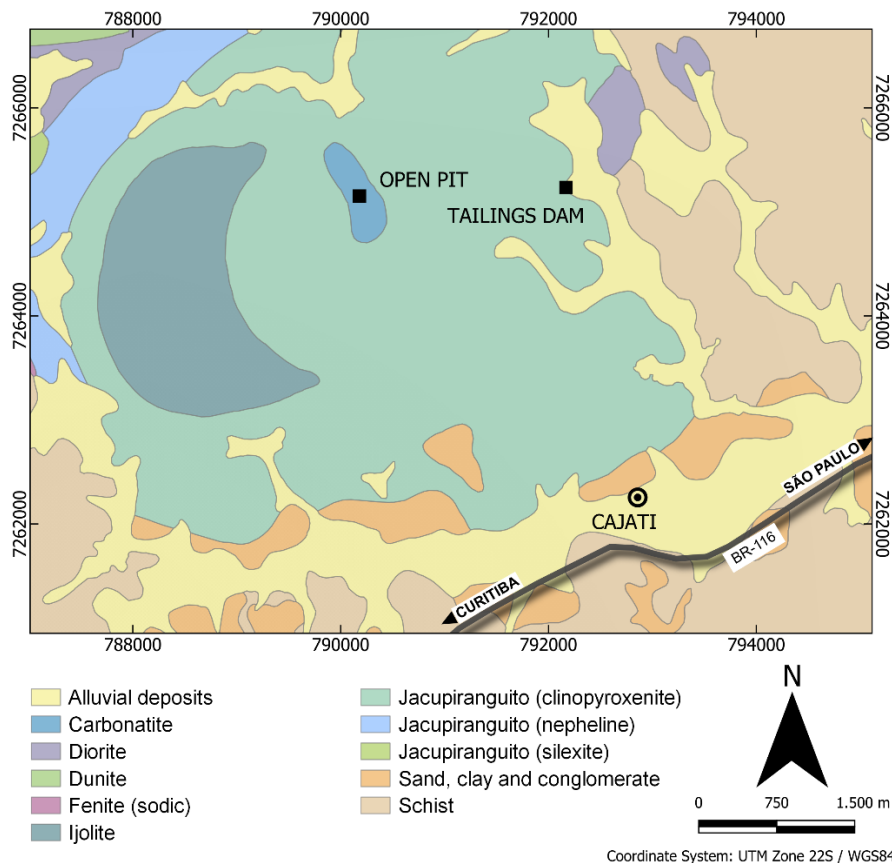


Figure 4 - Geological map of the Jacupiranga Alkaline Complex showing the open pit and tailings dam locations (modified from Faleiros & Pavan, 2013).

The main structural elements of carbonatites, such as joints, faults, dikes and fluid structures, are disposed in a radial and concentric aspect, suggesting an intrusive body from 5 successive intrusions that led to five different types of carbonatites, according to structural, mineralogical and petrographic features (Barros, 2001; Alves, 2008). Faria Junior et al. (2010) and Oliveira & Sant'Agostino (2020) cited the work developed by Saito et al. (2004) in the identification of a total of twelve geological units from the open pit, that considered not only geological characteristics but also relevant characteristics of the rock as ore in the beneficiation plant (Fig. 5).

Drilling has demonstrated that the carbonatites extend in depth to at least 400 m below the sea level, with a general dip angle of 80° , and the structures are mainly represented by a shear zone (fault), a set of joints and fractures (Alves, 2008). According to Oliveira & Sant'Agostino (2020), the fault zone corresponds to the main fault of a brittle shear regime that produced the main fault system and subsidiary faults, with N75W/subvertical direction.

Geotechnical structures

The main structures monitored by the microseismic system are the open pit and B1 DAM. Kuckartz (2017) stated that the bottom pit is located at approximately 170 m below the sea level, where the deepening of the pit is necessary to reach the annual production. The global angles of the current slopes (operational and future) are around 57° with benches height varying between 10 m and 20 m.

Since 1973, the dam has experienced nine raises (Fig. 6 and Table 1) with the maximum height of 44 m (at the level of the foundation) and 400 m crest length with 8 m width, a homogeneous starter dam composed by a compacted clay embankment with a rockfill downstream (Fig. 7) and volume of $1,258,444.56 \text{ m}^3$.

SEISMIC DESIGN CRITERIA AND STABILITY ANALYSIS

A reliable seismic slope stability analysis requires a relatively precise evaluation of seismic acceleration in the dam (Nimbalkar et al., 2018). Geotechnical

engineers usually perform tailing dam's stability analysis that employs a seismic coefficient under the load of a seismic event to calculate the factor of safety (Yener Ozkan, 1998; Singh et al., 2007; Sousa et al., 2021).

Pseudostatic method has long been customary, and it remains the workhorse for seismic stability analysis (Vick, 1990), in which the seismic coefficient is expressed in the value of acceleration that the structure is undergoing (Singh et al., 2007; Jibson, 2011; Nimbalkar et al., 2018). This method of analysis has the benefit of accumulated experience, reduced cost and user-friendliness, since it requires the estimation of a factor of safety in opposite to the seismic failure of the slopes of the earth structure (Bray & Travasarou, 2009; Jibson, 2011; Papadimitriou et al., 2014).

Mining geotechnical engineers generally use a pseudostatic approach to simulate the ground motion effect, through the definition of horizontal and vertical values of acceleration that can potentially unstable the structure.

Singh et al. (2007) stated that a potential sliding mass is irreversibly mobilized down slope, when ground acceleration in the down slope direction exceeds the threshold required to overcome the cohesive-frictional resistance at the base of the sliding mass, and the threshold acceleration above which the sliding mass is mobilized down slope, called yield acceleration.

Eletrobras' recommendations for seismicity criteria (yield acceleration) have been frequently used for tailings dams in Brazil (Schnaid & Mello, 2020). Eletrobras (2003) defines the values of $0.03g$ (3% of g) to vertical ($k_{v,g}$) and $0.05g$ (5% of g) to horizontal ($k_{v,h}$) components (Fig. 8), for a safety factor equal to 1.0 in pseudostatic analysis.

MICROSEISMIC MONITORING SYSTEM

Seismic sensors, array, and data acquisition

The sensor is the first, and arguably most important, component that seismic signals encounter as physical quantities are transduced from physical phenomena such as ground motion to a voltage, which is then sampled and ultimately ends up in electronic form in a database where

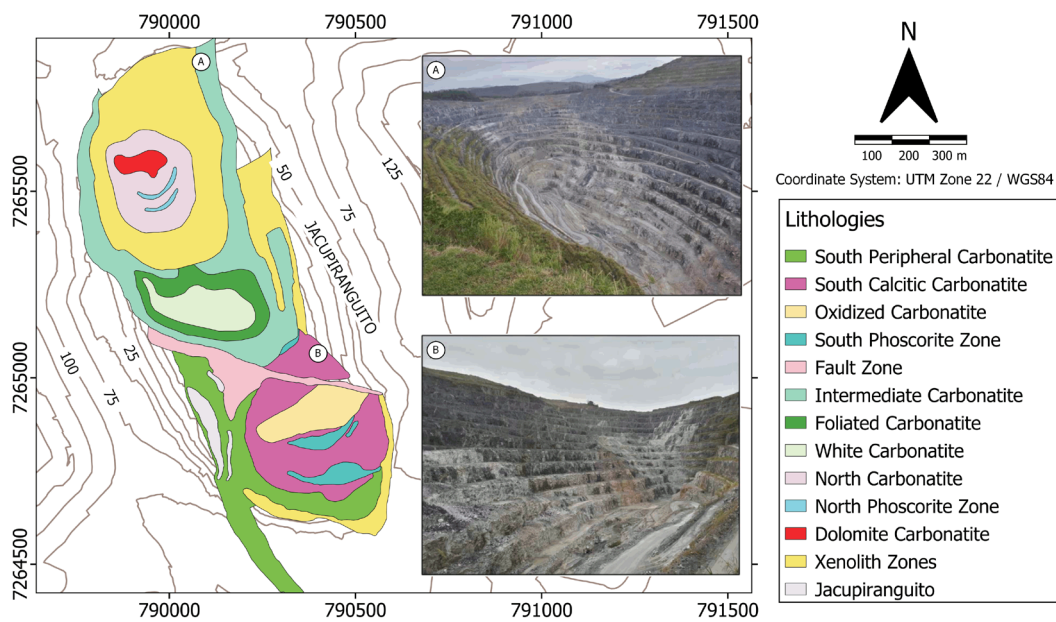


Figure 5 - Simplified geological map of carbonatitic bodies in the open pit (Saito et al., 2004; Faria Junior et al., 2010; Oliveira & Sant’agostino, 2020; Oliveira, 2021). (A) View from the North sector and (B) view from the South sector of the open pit.

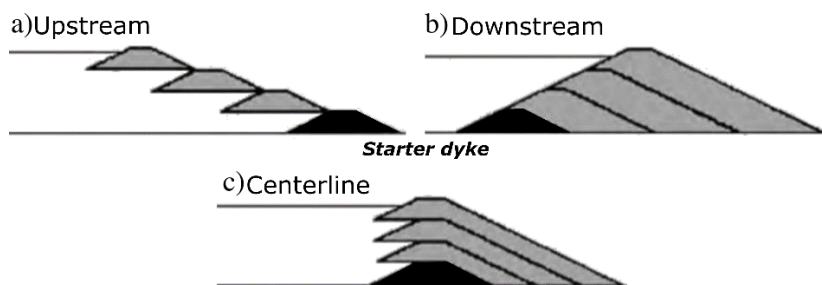


Figure 6 - Methods of construction: a) upstream, b) downstream and c) centerline (modified from Verdugo, 2009).

Table 1 – Dam’s raising over time (Oliveira, 2021).

Year	Stage	Height	Construction method
1973	Starter dam	49.1	
1992	1 st raise	52.1	Downstream
1995	2 nd raise	55.5	Downstream
1999	3 rd raise	60.5	Downstream
2003	4 th raise	65.0	Downstream
2008	5 th raise	66.0	Centerline
2009	6 th raise	71.0	Downstream
2013	7 th raise	72.0	Upstream
2015	8 th raise	73.0	Upstream
2018	9 th raise	75.0	Downstream

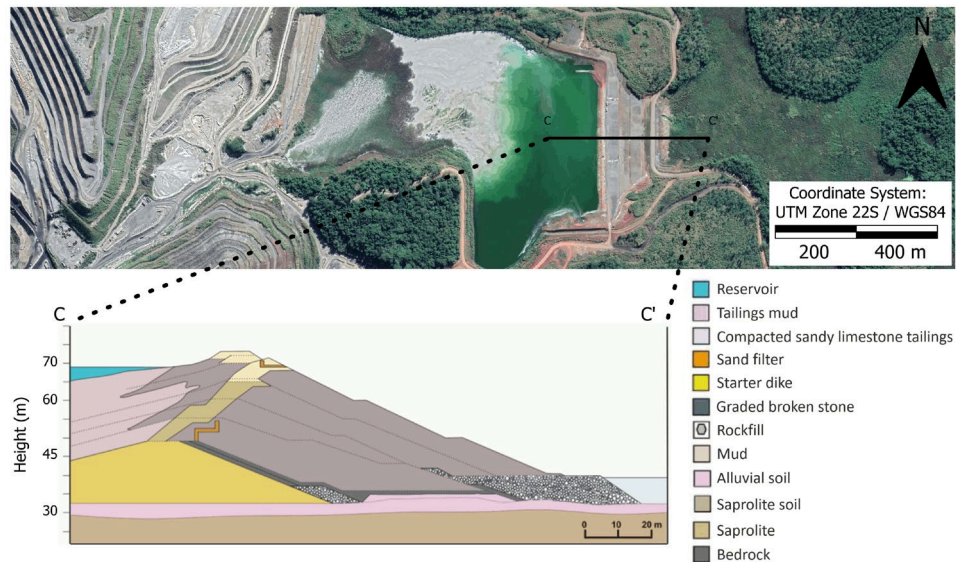


Figure 7 - Main cross-section of B1 Dam (modified from Oliveira, 2021) (image source from Google Earth 2020).

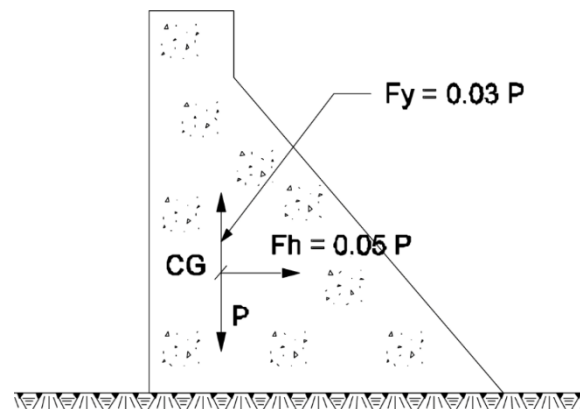


Figure 8 - Seismic forces in a dam (Eletrobras, 2003) where F_h and F_y correspond to the horizontal and vertical loadings, P represents the weight vector (inertial loadings), and CG is the total loading of the structure.

waveforms can be processed to build up a seismological catalog (Goldswain, 2020).

Geophones are preferred to accelerometers, since the typical frequencies recorded from slope seismic events are in the range of 10-400 Hz, in which geophones are more sensitive and reliable (Lynch & Malovichko, 2006). The sensors are connected to an analog-to-digital converter and the signal is then transmitted to a field seismic processor (powered by solar panels) for pre-processing, before the data are sent to an external seismic server through a radio or internet link. The field devices are coupled to a GPS to ensure the timing precision of each event recorded.

The Cajati microseismic array is comprised by 16 sensors located in the open pit (in the volume of rock behind the over-all pit slopes) and B1 Dam, where 12 triaxial geophones of 14 Hz were installed in depth boreholes of ~330 m covering the pit (two per hole) and 4 uniaxial geophones of 4.5 Hz were installed in shallow holes of ~50 cm in the dam crest (Fig. 9).

The main purpose of the open pit system is to monitor the changes in rock stability conditions, as a consequence of the blasts, due to the deepening of the pit for ore exploitation. The dam sensors aim to measure all operational ground motions that reach the embankment.

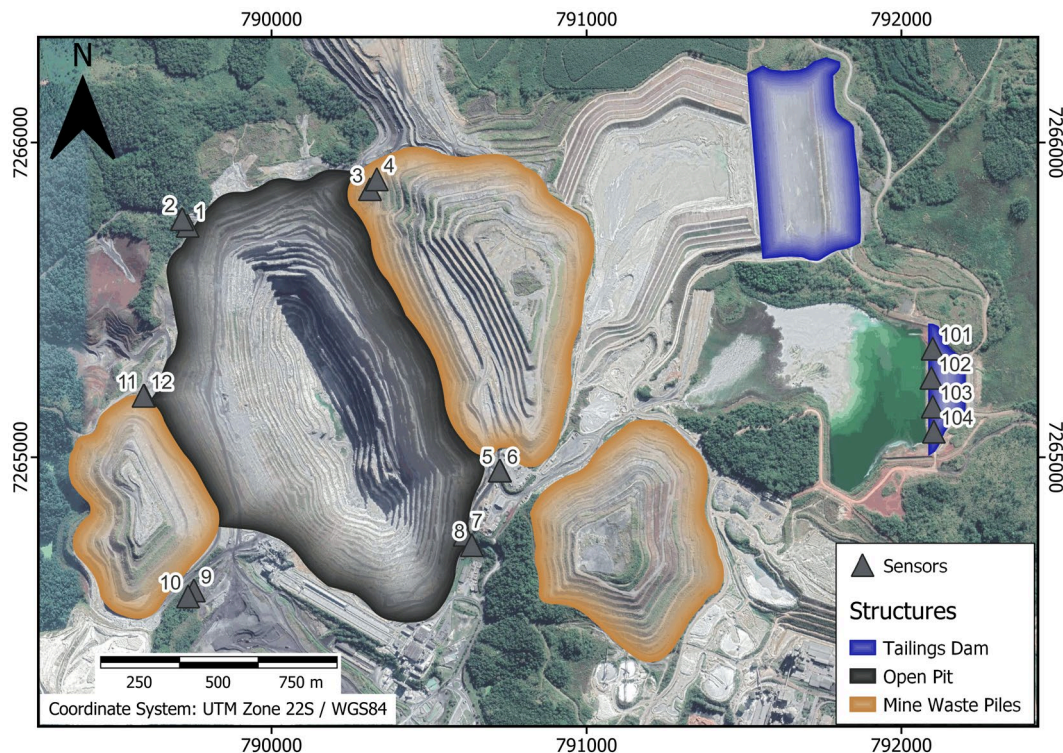


Figure 9 - Sensor array from the open pit (1 to 12) and tailings dam (101 to 104) (image Source from Google Earth 2020).

A seismic event is stored in the database when the system goes through the following stages: monitor each sensor continuously to decide when the signal becomes significant (triggering); ensure that the signal represents a seismic event (validation); decide which records from which sensors represent the same event (association); extract source and path parameters from the raw ground motion data for each event (seismological processing); and infer from a history of these parameters the processes which are taking place within a volume being monitored (interpretation) (Mendecki, 1997).

For all vibrations captured by the system, only the records that meet the triggering and association rules are stored in the database. To be considered a valid seismogram, an event needs to trigger a minimum of 4 geophones within a travel time tolerance of 0.1 seconds. The trigger level is reached when the ratio between STA (Short-Time Averages) / LTA (Long-Time Averages) is higher than 8. STA/LTA ratio is commonly used in seismology, when an event that exceeds a pre-set value is defined as “valid” and the data are recorded in the database.

Filtering and Discriminators

Once in the database, the events are classified (blast, event or noise) and processed (phase arrival picking). Depending on the outcome of the classification and the precision of the P and S-wave picking, the events are classified (manually or automatic) as either rejected or accepted. For this study, the database was queried to find events that were classified as blasts (Fig. 10) or natural seismicity.

The identification between seismograms generated by a blast or natural event (microseismic or microearthquake) was an important stage of the work. Ma et al. (2015) present some discriminating features, characteristics and procedures to discriminate blasts and microseismic events.

For each seismic event that was classified as blast, all seismograms were revisited and validated through some criteria like time of occurrence (blasts are well-timed events), waveform repetition (blasts are commonly characterized by a repetition of similar signals), E_S/E_P (ratio of S-wave energy to P-wave energy) and dominant frequency (blasts usually have higher frequency waves compared to natural seismic events).

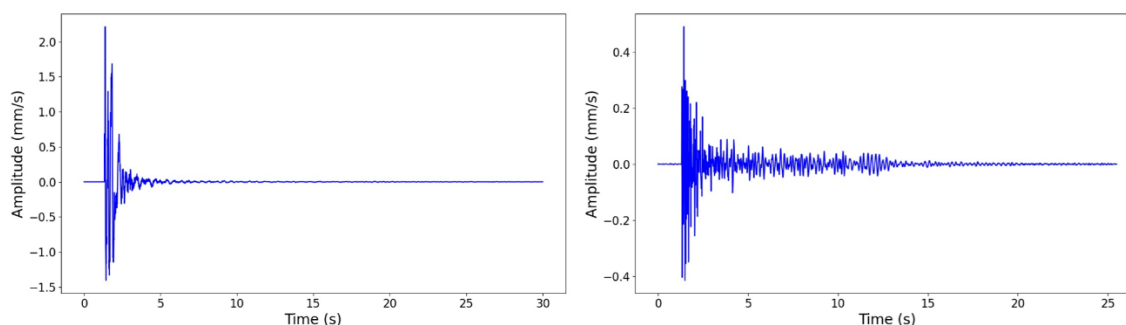


Figure 10 - Seismogram from the blast of August 18th, 2019, showing the waveform from the open pit (left) and tailings dam (right). The velocity peak is 5 times higher in the open pit with high attenuation. The dam waveform takes approximately 10 seconds for the vibrations completely dissipate (due to the seismic wave being trapped in the structure).

Blast timing was used as a temporal filtering in the database, where the time around 12:30pm / 3:30pm / 5:30pm was considered as potential blasts (based on the mining operation schedule). After the temporal filter, the presence of waveform repetition (as a consequence of the blast charge delays), the dominant frequency (excluding frequencies higher than 100 Hz) and the E_S/E_P ratio (it is expected that this ratio will be lower than 10) were investigated.

An extensive back analysis of all blasts and natural events registered by the open pit system for the period from April 24, 2018 to December 3, 2019 was performed. In this period we analyzed 450 blasts and 2,927 natural events from a total of 77,944 events and 318,893 seismograms in the database.

A second filter was applied to the data set, focusing on the selection of blasts that triggered sensors in the open pit and dam in the same time. This means that the selected events had enough energy to trigger sensors in the open pit and tailings dam, covering the distance of ~2 km between the structures in the time tolerance of 0.1 seconds. The total of 176 blast events were identified, producing 463 seismograms. The values of Peak Ground Velocity (PGV), Peak Ground Acceleration (PGA), % of g , period and dominant frequency were calculated for each seismogram.

MICROSEISMIC DATA ANALYSIS

Ground motion statistics and vibration standard

From the period analyzed, it was recorded 176 blasts that triggered sensors in the open pit and

tailings dam, recording 463 seismograms from ground motions noticed in the dam crest.

Values of PGV varied from 0.0023 to 0.4938 mm/s and PGA varied from 0.0007 (0.0070%) to 0.0847 m/s² (0.8661% of g , considering $g = 9.78$ m/s²). For PGV, the mean was 0.0871 mm/s and the median was 0.0673 mm/s, while for PGA, the mean was 0.0155 m/s² (0.2% of g) and the median was 0.0135 m/s² (0.1% of g). Table 2 and Figure 11 show the trigger statistics and value distribution for the period.

The top 5 values of PGA have higher frequency and are shown in Table 3. For all records, the dominant frequency ranges from 4.27 Hz to 38.46 Hz, the mean and median are 19.29 Hz and 19.23 Hz, and nearly 10% of the records are lower than 10 Hz. It is commonly understood that waves with higher frequency cause less damage due to the lower displacement produced. This is the reason for the frequency dependence of vibration standards, which shows that the structures can stand high ground motions with higher frequency.

Aloui & Bleuzen (2016) state that numerous studies have been performed to establish damage criteria for structures subjected to ground vibrations. Since the last two decades, PPV (Peak Particle Velocity) and frequency have been used as damage criteria for some standards like USBM (United States Bureau of Mines) and DIN (Deutsches Institut für Normung). The authors also stated that the potential damage to blast-induced vibrations on structures is conditioned by the particle velocity and the low-frequency portion of seismic waves. DIN 4150 considers critical the low frequencies (≤ 10 Hz) that exceed mm/s of PPV.

Table 2 - Sensor trigger statistics for events recorded by the system.

Sensor	Number of triggers	Maximum PGV (mm/s)	Mean PGV (mm/s)	Maximum PGA (m/s ²)	Mean PGA (m/s ²)
All	463	0.4938	0.0871	0.0847	0.0154
101	121	0.1608	0.0513	0.0230	0.0079
102	142	0.4938	0.1194	0.0847	0.0219
103	117	0.4909	0.1041	0.0841	0.0184
104	83	0.1820	0.0601	0.0368	0.0112

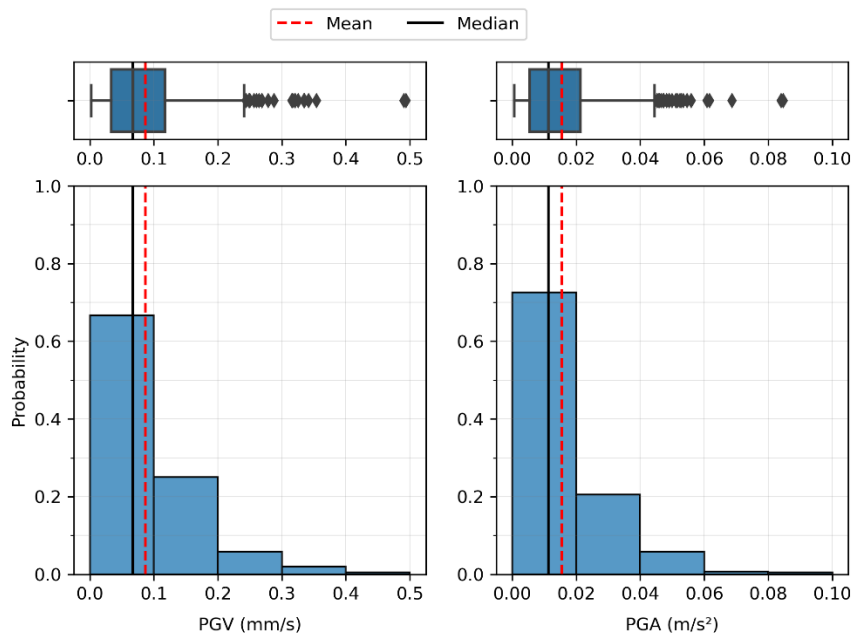


Figure 11 – Distribution of trigger records in a box-plot diagram and estimated frequency distribution for the whole period.

Table 3 - Top 5 PGA from the dam sensors.

PGA [m/s ²]	PGA [% of g]	Frequency (Hz)	Date	Hour	Sensor
0.0847	0.8661	18.52	08/20/2019	12:23:47pm	102
0.0841	0.8599	14.29	08/20/2019	12:23:47pm	103
0.0687	0.7025	26.32	11/14/2018	12:37:42pm	102
0.0616	0.6299	25.00	01/31/2019	07:18:15am	102
0.0609	0.6227	33.33	10/01/2018	05:45:13pm	103

The analysis involving vibration limits, as used in civil engineering projects, can also be applied as evident from the German standard DIN 4150 (Kouroussis et al., 2014). This standard makes a relationship between the PPV and the frequency of an event, for three levels of structures, defined as L1 (industrial and commercial purpose buildings), L2 (dwellings) and L3 (structures sensitive to dynamics effects).

The PPV refers to the highest resultant value measured for each component of a sensor, in the case of triaxial ones, where the PGV is the highest absolute value among those recorded by all sensor components. As the geophones in the dam are uniaxial, the PGV and PPV are equal for the vertical direction. Figure 12 shows a comparison between vertical vibrations of the dams and the L3 level of DIN 4150. It presents that the lower values of PGV (0.0011 mm/s – 0.4938 mm/s) with higher frequency (>10 Hz) are far from the limit defined for structures sensitive to dynamics effects.

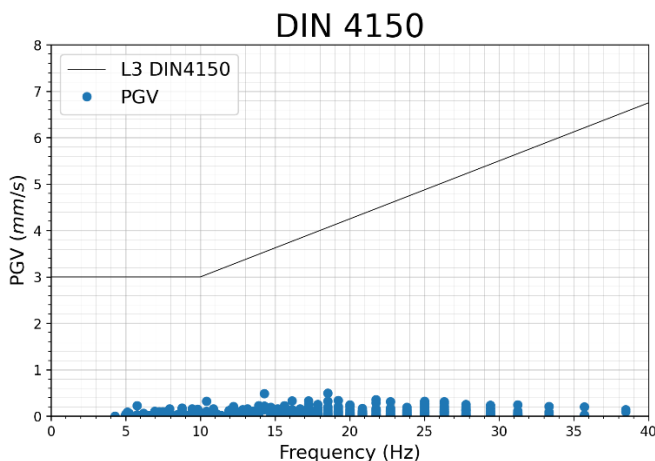


Figure 12 - Vertical vibrations of the sensors in the dam relating to L3 level of DIN 4150.

Other analysis

From the 176 blasts filtered, 26 blasts were manually processed and accepted as a valid event to estimate the source parameters. The blast's source parameters considered events where the signal-to-noise ratio was large enough to accurately pick P and S-waves.

The source parameters allow the estimations of the event magnitude (of local and moment), potency, seismic energy and E_s/E_p . Table 4 shows the source parameter from the highest PGA

measured with its location (Fig. 13). The blast of August 20, 2019, generated a ground motion with the highest PGA value of 3.1343 m/s^2 (32.04% of g in sensor 6) in the open pit with the lowest values of 0.0841 m/s^2 (0.8599% of g in sensor 103) in the dam crest at a distance of $\sim 1.6 \text{ km}$ from the epicenter, indicating high attenuation, especially for high frequencies, likely due to loose material used in the dam embankment.

Table 4 - Source parameters of the event with the highest PGA.

Date	08/20/2019
Hour	12:23:47pm
Local Magnitude	1.9
Moment Magnitude	2.3
Potency (m^3)	1.1×10^2
Energy (J)	19.1×10^5
Energy Ratio (E_s/E_p)	0.5
PGA (m/s^2)	0.0847

From the top 10 values of PGA, 5 events were manually processed with large enough signal noise ratio where P and S-waves were accurately picked. This comparison is shown in Table 5, and the source location of the top 5 manually processed blasts is shown in Figure 14. The high value of the E_s/E_p ratio for one event was likely due to probably surface wave contamination. As blasts are predominantly producing P-waves, it is expected that this ratio will be lower than 10.

BLAST GROUND MOTION ASSESSMENT

The highest ground motion value measured at the dam was 3.46 times lower than the vertical coefficient of 3% (0.03g) defined by the Eletrobras standard. The whole database showed that nearly 95% of the values are lower than 0.06 m/s^2 (0.6135% of g) with 90% of the records with higher dominant frequency that presents reduced damage potential due to the lower capacity to produce high values of displacement, and consequently the capacity to reach safety factor less than 1 for a pseudostatic analysis that considered Eletrobras values as seismic criteria.

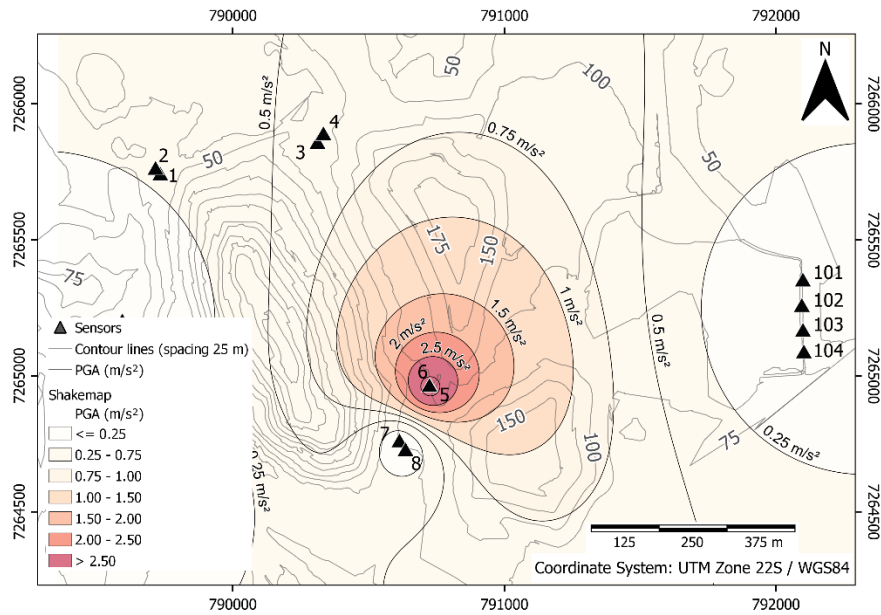


Figure 13 - Colored shake map in PGA (m/s^2) from the highest ground motion detected by sensor 6 (first to be triggered) with $3.1343 m/s^2$, reaching the dam with $0.0847 m/s^2$ and $0.0841 m/s^2$ in sensors 102 and 103.

Table 5 - Source parameters of the top 5 events manually processed with higher values of PGA in the dam.

Date	08/20/2019	09/22/2018	12/01/2019	01/21/2019	02/06/2019	08/01/2019
Hour	12:23:47pm	12:21:58pm	12:57:43pm	03:13:50pm	05:27:58pm	05:20:32pm
Local Magnitude	1.9	1.1	1.2	2.0	1.0	1.6
Moment Magnitude	2.3	1.4	1.7	2.2	1.7	1.7
Potency (m^3)	1.1×10^2	5.1	12	73	12	13
Energy (J)	9.1×10^5	3.8×10^5	1.7×10^5	2.2×10^6	3.8×10^4	3.1×10^6
Energy Ratio (E_S/E_P)	0.5	1.3	6.9	0.5	3.6	19.5
PGA (m/s^2)	0.0847	0.0482	0.0343	0.0524	0.0473	0.0560

The dam trigger statistics presented in Table 2 showed that the sensors in the middle of the embankment crest and close to the left abutment were 1.4 to 1.7 times more triggered than the ones close to the right abutment. The sensors located closer to the center of the structure, 102 and 103, presented values of the PGV and PGA means, on average, 2 times higher than the sensors close to the left and right abutment. This indicates possible ground motion amplification in the middle of the dam embankment, which is likely related to the greater thickness of the loose fill material which is expected to have low seismic wave speeds (Olivier et al., 2018). This phenomenon is common

in crustal seismology, where sedimentary basins (low velocity zones) can result in significant site amplification for large earthquakes (e.g. Graves et al., 1998).

It is important to mention that the local geology, as an intervening factor, has an important role in the highest attenuation observed from the epicenter and ground motions recorded in the dam embankment, approximately 2 km far from the open pit. In the highest blast PGA measured by the system, the accelerations had a wide drop, from 32.04% (epicenter) to 0.8599% (dam).

Seismic data can be used to assess blast's efficiency, whilst ensuring that PGA or PGV does

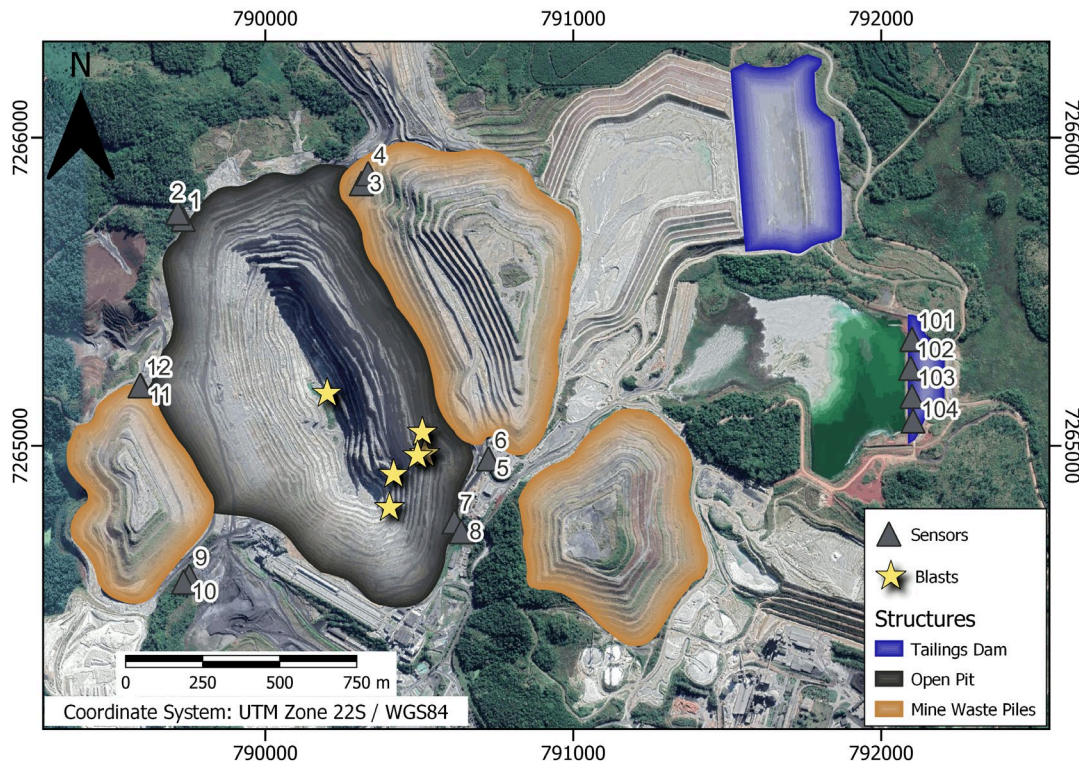


Figure 14 - Location of the top blasts (yellow stars) manually processed (image source from Google Earth 2020).

not exceed the dam's design criteria. If the blasts' information could be acquired, the microseismic monitoring would calibrate a relationship between charge weights and the ground motions recorded at the dam. This analysis would enable geotechnical and mining engineers to plan the charge of the blasts in a way to keep ground motion accelerations lower than that established in the pseudostatic analysis.

The manually processed blasts analyzed have shown that the local magnitudes (ML) varied from 1.0 to 2.0 and the seismic energy varied from 3.8×10^4 J to 3.1×10^6 J, with the highest PGA event at a distance of approximately 1.6 km from the dam. The current blast conditions, like geometric parameters dimensioning, charge weight and detonation timing, are generating vibrations much lower than the ones obtained from technical standard values of acceleration (Eletrobras) or PGV (DIN 4150).

The adoption of technical standard values as safety criteria can support the search for optimum values of explosive charge weight, which can be used per delay without exceeding the safe limit of the ground vibration.

CONCLUSION

A routine microseismic monitoring system can support geotechnical engineers to measure the vibrations that reach tailings dams and compare them with design criteria parameters, like seismic coefficient of pseudostatic analysis. The monitoring also gathers a new type of dataset that complements the current instrumentation used in the geotechnical monitoring of dams' operation, as well as a support method to assess potential liquefaction when the vibration data are correlated with water level and piezometric data.

For the period analyzed, the B1 Dam did not experience high values of PGA and PGV. When this period is compared with Brazilian and German standards, it shows that the blasts-induced seismicity is not prone to cause damage to the dam.

The source parameters estimated can give valuable information about the blast efficiency and can be used to improve mine operations and create control criteria (TARP) to keep the vibrations in a certain level that do not affect the dam safety integrity.

Based on the seismic source parameter estimation, it is well-known that blasts are human

controlled events, with known location, charge weight and source time. Normally, depending on signal-to-noise ratio conditions, it is possible to obtain the seismic source parameters like magnitude and seismic energy that can be related to the blast's design.

These results cannot be extrapolated to other mining operations since the design of mine elements, as the pit location, mine waste pile distribution, and dams' location can vary a lot as well as the seismic design criteria of each cited structure.

ACKNOWLEDGMENTS

The authors would like to thank Mosaic Fertilizantes Company, in the name of Luís Antonio Pinto e Almeida and Ricardo Luiz Teixeira Telles, for allowing the use of the database and all support in the development of this work, Tetra Tech and IMS (Institute of Mine Seismology) in Australia for all support, Daniel Coelho, Felipe Jesus, Victor Salles and Matheus Cunha for the discussions and coding.

REFERENCES

- ALOUÏ, M.; BLEUZEN, Y. 2016. Ground Vibrations and Air Blast Effects Induced by Blasting in Open Pit Mines: Case of Metlaoui Mining Basin, Southwestern Tunisia. *Journal of Geology & Geophysics*, 5(3): 8 pp.
- ALVES, P. R. 2008. The carbonatite-hosted apatite deposit of Jacupiranga, SE Brazil: styles of mineralization, ore characterization and association with mineral processing. Master thesis -Missouri: Missouri University of Science and Technology, 140 pp.
- BARROS, G. 2001. Reavaliação Geoestatística dos Recursos/Reservas de Fosfato da Mina de Cajati, SP. Master thesis – SP, Brazil: Universidade de São Paulo, 121 pp.
- BRAY, J. D.; TRAVASAROU, T. 2009. Pseudostatic Coefficient for Use in Simplified Seismic Slope Stability Evaluation. *Journal of Geotechnical and Geoenvironmental Engineering*, 135(9): 1336–1340.
- DIAS, L. S. O.; OLIVIER, G.; ARAÚJO, R. N.; BARBOSA, M. R.; BRANDI, I.; FERREIRA, M. L.; BRAGA, M. A. d. S.; GOMES, R. C. 2016. A microseismic monitoring pilot project of natural caves in Carajás – PA. Proceedings of the 7th Simpósio Brasileiro de Geofísica. Ouro Preto, MG, Brazil. SBGf.
- ELETROBRAS. 2003. Critérios de Projeto Civil de Usinas Hidrelétricas - Eletrobras - Centrais Elétricas Brasileiras S.A. [s.l.] Eletrobras, RJ, Brazil, 278 pp.
- ERRINGTON, A. 2006. Sensor Placement for Microseismic Event Location. Master thesis - Saskatoon, Canada: University of Saskatchewan, 87 pp.
- FALEIROS, F. M.; PAVAN, M. 2013. Geologia e recursos minerais da Folha Eldorado Paulista – SG.22-X-B-VI, Estado de São Paulo, Escala 1:100.000. São Paulo, Brazil. CPRM, p. 128.
- FARIA JUNIOR, A.; TOMI, G.; SANT'AGOSTINO, L. M.; COSTA, J. F. C. L. 2010. O impacto do tipo de amostragem no controle de qualidade na lavra. *Rem: Revista Escola de Minas*, 63(2): 385–392.
- GOLDSWAIN, G. 2020. Advances in seismic monitoring technologies. Proceedings. In: Second International Conference on Underground Mining Technology. Australian Centre for Geomechanics, Perth, Australia.
- GOOGLE EARTH. 2020. [Online] Available at: <<http://www.google.com/earth/index.html>> Access on: August 10, 2020.
- GRAVES, R. W.; PITARKA, A.; SOMERVILLE, P. G. 1998. Ground-Motion Amplification in the Santa Monica Area: Effects of Shallow Basin-Edge Structure. *Bulletin of the Seismological Society of America*, 88: 1224-1242.
- JIBSON, R.W. 2011. Methods for assessing the stability of slopes during earthquakes – A retrospective. *Engineering Geology*, 122(1–2): 43–50
- KOUROUSSIS, G.; CONTI, C.; VERLINDEN, O. 2014. Building vibrations induced by human activities: a benchmark of existing standards. *Mechanics & Industry*, 15(5): 345–353.
- KUCKARTZ, B. T. 2017. Análise da expansão da cava com múltiplas restrições de superfície sob incerteza geológica. Master Thesis. Universidade Federal do Rio Grande do Sul, RS, Brazil. 159 pp.
- LIJIE, G. Micro Seismic Monitoring Technique and Practice of Rock Blast in Deep Mining. *Electronic*

- Journal of Geotechnical Engineering, 20: 4587–4596, 2015.
- LIMA, R. E.; PICANÇO, J. d. L.; SILVA, A. F.; ACORDES, F. A. 2020. An anthropogenic flow type gravitational mass movement: the Córrego do Feijão tailings dam disaster, Brumadinho, Brazil. *Landslides*, 17(12): 2895–2906.
- LYNCH, R. A.; MALOVICHKO, D. A. 2006. Seismology and slope stability in open pit mines. In: *International Symposium on Stability of Rock Slopes. Proceedings... Southern Africa Institute of Mining and Metallurgy Johannesburg*.
- MA, J.; ZHAO, G.; DONG, L.; CHEN, G.; ZHANG, C. 2015. A Comparison of Mine Seismic Discriminators Based on Features of Source Parameters to Waveform Characteristics. *Shock and Vibration*, 2015: 10 pp.
- MA, K.; DONG, L.; ZHAO, G.; LI, X. 2017. Stability analysis and reinforcement evaluation of high-steep rock slope by microseismic monitoring. *Engineering Geology*, 218: 22–38.
- MENDECKI, A. J. 1997. *Seismic monitoring in mines*. London, UK: Chapman & Hall, 273 pp.
- MENDECKI, A. J.; LYNCH, R. A.; MALOVICHKO, D. A. 2010. Routine Micro-Seismic Monitoring in Mines. *Australian Earthquake Engineering Society 2010. Proceedings...Perth, Western, Australia*.
- NIMBALKAR, S.; ANNAPAREDDY, V. S. R.; PAIN, A. 2018. A simplified approach to assess seismic stability of tailings dams. *Journal of Rock Mechanics and Geotechnical Engineering*, 10(6): 1082–1090.
- OLIVEIRA, L. A. 2021. Caracterização e monitoramento de barragens de rejeito através de métodos geofísicos. Master thesis. Universidade Federal do Rio de Janeiro, RJ, Brazil. 187 pp.
- OLIVEIRA, S. B.; SANT'AGOSTINO, L. M. 2020. Litho geochemistry and 3D geological modeling of the apatite-bearing Mesquita Sampaio befor site, Jacupiranga alkaline complex, Brazil. *Brazilian Journal of Geology*, 50(3): e20190071. 11 pp.
- OLIVIER, G.; BRENGUIER, F.; WIT, T. de; LYNCH, R. 2017. Monitoring the stability of tailings dam walls with ambient seismic noise. *The Leading Edge*, 36(4): 72–79.
- OLIVIER, G.; WIT, T. de; BRENGUIER, F.; KUNJWA, T. 2018. Ambient noise Love wave tomography at a gold mine tailings storage facility. *Géotechnique Letters*, 8(3): 178–182.
- OZKAN, M. Y. 1998. A review of considerations on seismic safety of embankments and earth and rock-fill dams. *Soil Dynamics and Earthquake Engineering*, 17(7–8): 439–458.
- PAPADIMITRIOU, A. G.; BOUCKOVALAS, G. D.; ANDRIANOPOULOS, K. I. 2014. Methodology for estimating seismic coefficients for performance-based design of earthdams and tall embankments. *Soil Dynamics and Earthquake Engineering*, 56: 57–73.
- SAITO, M. M.; BARROS, M. M.; BONÁS, T. B.; BETTENCOURT, J. S. 2004. Mapeamento geológico de detalhe da mina Cajati (SP): Modelo conceitual e aplicação à lavra, produção e beneficiamento. In: *XLIV Congresso Brasileiro de Geologia. Proceedings. Araxá, MG, Brazil: Sociedade Brasileira de Geologia*.
- SCHNAID, F.; MELLO, L. G. F. S. 2020. Guidelines and recommendations on minimum factors of safety for slope stability of tailings dams. *Soils and Rocks*, 43(3): 369–395.
- SHURAN, L.; SHUJIN, L. 2011. The Discussion about the Safety Management of the Mine Tailings Pond near the Mine Stope. *Procedia Engineering*, 26: 1901–1906.
- SILVA, R. A. 2019. Geofísica aplicada à caracterização da barragem de rejeito de mineração B1, Cajati, São Paulo. Master thesis, Universidade Federal do Rio de Janeiro, RJ, Brazil. 80 pp.
- SILVA-CASTRO, J. J. 2012. Blast vibration modeling using improved signature hole technique for bench blast. Master thesis - Lexington, Kentucky: University of Kentucky, 236 pp.
- SINGH, R.; ROY, D.; DAS, D. 2007. A correlation for permanent earthquake-induced deformation of earth embankments. *Engineering Geology*, 90(3–4): 174–185.
- SOUSA, G. M. DE; FERREIRA, S. A.; GOMES, R. C. 2021. Methodology for automated monitoring of induced vibrations in tailings dams built upstream. *Geotechnical and Geological Engineering*, preprint. DOI: 10.21203/rs.3.rs-162752/v1
- VERDUGO, R. 2009. Seismic performance based-design of large earth and tailing dams. In: KOKUSHO, T.; TSUKAMOTO, Y.; YOSHIMINE, M. (Eds.). *Performance-Based Design in*

Earthquake Geotechnical Engineering. Taylor & Francis Group, London, CRC Press. p. 41–60.

VICK, S. G. 1990. Planning, design, and analysis of tailings dams. Vancouver, B.C., Canada: BiTech Publishers, 381 pp.

WIT, T.; OLIVIER, G. 2018. Imaging and monitoring tailings dam walls with ambient seismic noise. In: 21st International Seminar on Paste and Thickened Tailings. Available on: <https://papers.acg.uwa.edu.au/p/1805_37_de_Wit/>. Access on: December 11, 2021.

L.S.O.D.: responsible for writing the article, as a result of the doctoral research in geology at UFRJ. **M.A.B:** advisor of the research work. Contributed to the planning of the study, guided the analyses, methodology and the products developed, results, discussions and conclusions, review and writing of parts of the article. **A.S.C.:** contributed to the analysis, results, discussions and conclusions, definition of figures, review and writing of parts of the article. **G.O.:** co-advisor of the research work. Contributed to the creation of some images and data processing, review and writing of parts of the article. **R.P.F.:** co-advisor of the research work. Contributed to the discussions and conclusions of the work, bibliography and review of the article.

Received on December 18, 2021 / Accepted on April 28, 2022